JOURNAL OF VIROLOGY, Nov. 2006, p. 10315–10324 Vol. 80, No. 21
0022-538X/06/$08.00+0 doi:10.1128/JVI.01138-06

Identifying Epitopes Responsible for Neutralizing Antibody and DC-SIGN Binding on the Spike Glycoprotein of the Severe Acute Respiratory Syndrome Coronavirus

Yi-Ping Shih,[1,2] Chia-Yen Chen,[1,2] Shih-Jen Liu,[3] Kuan-Hsuan Chen,[1] Yuan-Ming Lee,[2,4] Yu-Chan Chao,[5] and Yi-Ming Arthur Chen[1,2]*

AIDS Prevention and Research Center, National Yang-Ming University,[1] Division of Preventive Medicine, Institute of Public Health, School of Medicine National Yang-Ming University,[2] Vaccine Research and Development Center, National Health Research Institutes,[3] Department of Pathology and Laboratory Diagnosis, Taipei Veterans General Hospital,[4] and Institute of Molecular Biology, Academia Sinica,[5] Taipei, Taiwan, Republic of China

Received 2 June 2006/Accepted 5 August 2006

The severe acute respiratory syndrome-associated coronavirus (SARS-CoV) uses dendritic cell-specific ICAM-3 grabbing nonintegrin (DC-SIGN) to facilitate cell entry via cellular receptor-angiotensin-converting enzyme 2. For this project, we used recombinant baculoviruses expressing different lengths of SARS-CoV spike (S) protein in a capture assay to deduce the minimal DC-SIGN binding region. Our results identified the region location between amino acid (aa) residues 324 to 386 of the S protein. We then generated nine monoclonal antibodies (MAbs) against the S protein to map the DC-SIGN-binding domain using capture assays with pseudotyped viruses and observed that MAb SIa5 significantly blocked S protein–DC-SIGN interaction. An enhancement assay using the HKU39849 SARS-CoV strain and human immature dendritic cells confirmed our observation. Data from a pepscan analysis and M13 phage peptide display library system mapped the reactive MAb SIa5 epitope to aa residues 363 to 368 of the S protein. Results from a capture assay testing three pseudotyped viruses with mutated N-linked glycosylation sites of the S protein indicate that only two pseudotyped viruses (N330Q and N357Q, both of which lost glycosylation sites near the SIa5 epitope) had diminished DC-SIGN-binding capacity. We also noted that MAb SIb4 exerted a neutralizing effect against HKU39849; its reactive epitope was mapped to aa residues 435 to 439 of the S protein. We offer the data to facilitate the development of therapeutic agents and preventive vaccines against SARS-CoV infection.

Severe acute respiratory syndrome (SARS) causes progressive respiratory failure and death in approximately 10% of infected individuals (14, 35). A SARS-associated coronavirus (SARS-CoV) has been identified as the causal agent (15, 17, 26, 35), and angiotensin-converting enzyme 2 (ACE2) and dendritic cell-specific ICAM-3 grabbing nonintegrin (DC-SIGN) have been identified as SARS-CoV cellular receptors (30, 33, 44).

The SARS-CoV spike (S) protein is 1,255 amino acids (aa) in length; its 43 strains share 97.7% sequence identity (28). It contains two domains—SI (aa residues 17 to 680) and SII (aa residues 681 to 1,255)—which are, respectively, responsible for receptor binding and membrane fusion (38, 40). The receptor binding domain (aa residues 318 to 510) of the S protein contains a major neutralization determinant capable of inducing potent neutralizing antibodies in mice (22). A recombinant protein (RP) containing aa residues 310 to 510 of the S protein absorbs and removes most neutralizing antibodies in various animals inoculated with a modified vaccinia virus Ankara that expresses a full-length S protein (8). According to these findings, SARS-CoV S protein receptor binding domain is a critical target for vaccine and therapeutic pharmaceutical development.

DC-SIGN, a C-type lectin receptor expressed on dendritic cells (DCs), was initially identified as a human immunodeficiency virus (HIV) attachment factor (13, 18) but has since been found to be a receptor for hepatitis C virus (36), Ebola virus (2), cytomegalovirus (21), dengue virus (41), and other viruses. In addition to enhancing viral infections in target cells (16, 18, 27), in some cases, DC-SIGN also serves as a receptor for virus replication in dendritic cells (2, 41). Besides, a DC-SIGN-related molecule called L-SIGN (DC-SIGNR, liver and lymph node specific, CD209L), which mainly expresses in the lymph node and liver sinusoidal endothelial cells (3, 39), has a function similar to that of DC-SIGN for virus-cell interaction (2, 3, 32, 34). Previously, several studies demonstrated that both DC-SIGN and L-SIGN can bind SARS-CoV S protein and facilitate virus dissemination (4, 23, 33, 44). However, the domains on the S protein responsible for the binding of DC-SIGN have not been elucidated.

In this study, we used recombinant baculoviruses expressing different S protein lengths with a standard capture assay to identify the minimal DC-SIGN binding region of the S protein and then generated a panel of monoclonal antibodies (MAbs) against the S protein to map the DC-SIGN-binding and ACE2-binding domains using pseudotyped viruses. Our results were confirmed using the SARS-CoV strain HKU39849 in a culture system with human immature DCs. The epitopes of MAbs that expressed the neutralizing effect were mapped using pepscan and M13 phage display library-screening methods. The results

* Corresponding author. Mailing address: AIDS Prevention and Research Center, National Yang-Ming University, Taipei 111, Taiwan, Republic of China. Phone: 886 2 28267304. Fax: 886 2 28270576. E-mail: arthur@ym.edu.tw.

indicate ACE2 and DC-SIGN recognition of distinct SI domain epitopes.

MATERIALS AND METHODS

SARS-CoV strain, recombinant baculoviruses, and pseudotyped viruses. A SARS-CoV HKU39849 strain (GenBank accession no. AY278491) (45) was used in the infection and DC-SIGN-mediated assays. To determine the minimal region of the S protein interacting with DC-SIGN, a panel of recombinant baculoviruses (vAtEpG280, vAtEpG324, vAtEpG386, vAtEpG434, vAtEpG488, and vAtEpG763) containing different lengths of S protein were used in the capture assay. The peptide sequences of S protein fused to the truncated gp64 of the following baculoviruses were 17 to 280 aa for vAtEpG280, 17 to 324 aa for vAtEpG324, 17 to 386 aa for vAtEpG386, 17 to 434 aa for vAtEpG434, 17 to 488 aa for vAtEpG488, and 17 to 763 aa for vAtEpG763 (5). All of the recombinant baculoviruses contain the enhanced green fluorescent protein (EGFP) for easy detection. Pseudotyped viruses expressing SARS-CoV S protein were generated by cotransfecting HEK293T cells with plasmid DNAs from pNL-Luc-E$^-$R$^-$ and any one of the following plasmids: pcDNA3-S (30), pcDNA3-SN65Q, pcDNA3-SN330Q, pcDNA3-SN357Q, or pcDNA3-SN330Q+SN357Q. Plasmid pNL-Luc-E$^-$R$^-$ contains a defective HIV type 1 (HIV-1) genome with a firefly luciferase reporter gene (11), and the construction of plasmids will be presented in the next section. For transfection experiments, 2.5×10^6 HEK293T cells were seeded 1 day before transfection in a 10-cm plate. Forty-eight hours after transfection, the culture supernatants were harvested, filtered through a 0.45-μm filter (Millipore, Bedford, MA), and concentrated by ultracentrifugation to one-third of the original volume. The concentrations of the pseudotyped viruses were determined using an HIV-1 p24 assay (Beckman Coulter, Somerset, N.J.), and the viral stocks (80 ng of p24/ml) were aliquoted and frozen at −80°C.

Mutagenesis of N-linked glycosylation sites of S protein. A plasmid pcDNA3-S which contains a codon-optimized S gene of SARS-CoV was kindly provided by M. Farzan (30). To mutate the N-linked glycosylation sites from Asn to Gln, a QuikChange II XL site-directed mutagenesis kit (Stratagene, La Jolla, CA) was used. The following three pairs of primers were used to generate pcDNA3-SN65Q, pcDNA3-SN330Q, pcDNA3-SN357Q, and pcDNA3-SN330Q+SN357Q plasmids, respectively: FN65, 5′-CTGCCCTTCTACTCCCA AGTGACCGGCTTCCAC-3′; RN65, 5′-GTGGAAGCCGGTCACTTGGGAG TAGAAGGGCAG-3′; FN330, 5′-CGGCGAGGTGTTCCAAGCCACCAAGT TCCC-3′; RN330, 5′-GGGAACTTGGTGGCTTGGAACACCTCGCCG-3′; FN357, 5′-GATTATAGCGTGCTGTATCAAAGCACCTTTTTTAGCACC-3′; RN357, 5′-GGTGCTAAAAAAGGTGCTTTGATACAGCACGCTATAATC-3′. All of the plasmids were confirmed by sequencing using a dye terminator cycle sequencing core kit on a DNA sequencer (Applied Biosystems).

Cell lines and cell culture. The following five cell lines were used in this study: HepG2 is a human hepatoblastoma cell line (1), Vero E6 is an African Green monkey kidney cell line (25), HEK293T is a human kidney cell line (19), B-THP-1 is a Raji B cell line, and B-THP-1/DC-SIGN is a stable clone of B-THP-1 expressing DC-SIGN (43). HepG2, Vero E6, and HEK293T cell lines were cultured in Dulbecco's modified Eagle's medium (GIBCO-BRL, Grand Island, NY) supplemented with 10% heat-inactivated fetal bovine serum (HyClone, Logan, Utah), penicillin (100 U/ml), streptomycin (100 μg/ml), nonessential amino acids (0.1 mM), and L-glutamine (2 mM) (GIBCO-BRL). B-THP-1 and B-THP-1/DC-SIGN cells were cultured in RPMI 1640 medium (GIBCO-BRL) supplemented with 10% heated-inactivated fetal calf serum, penicillin (100 U/ml), and streptomycin (100 μg/ml). For the B-THP-1/DC-SIGN cell line, 50 μg/ml of neomycin (Sigma-Aldrich, St. Louis, MO) was added to the medium.

Preparation of human immature DCs. Peripheral blood mononuclear cells were isolated from a healthy donor by standard density gradient centrifugation with Ficoll-Paque (Amersham Biosciences, Piscataway, NJ). CD14$^+$ cells were subsequently purified from peripheral blood mononuclear cells through high-gradient magnetic sorting by using VARIOMACS technique with anti-CD14 microbeads (Miltenyi Biotec GmbH, Bergisch Gladbach, Germany). Human CD14$^+$ monocytes (5×10^5 cells/ml) were cultivated in RPMI 1640 medium supplemented with 10% fetal calf serum, 800 U/ml human granulocyte-macrophage colony-stimulating factor (R&D Systems, Minneapolis, MN), and 500 U/ml human interleukin-4 (R&D) for 6 days to differentiate into immature DCs.

DC-SIGN-mediated capture assay and enhancement assay. The standard capture assay has been described previously (18, 32). Briefly, B-THP-1 cells, B-THP-1/DC-SIGN cells, or immature DCs were incubated with SARS-CoV (HKU39849 strain) (50 50% tissue-culture infectious doses [$TCID_{50}$]), recombinant baculoviruses (multiplicity of infection [MOI] of 10) or pseudotyped viruses (equivalent to 4 ng p24) at 37°C for 2 h. The cells were then washed with RPMI 1640 twice before they were added to the target cells (Vero E6 or HepG2 cells). For the DC-SIGN-mediated enhancement assay, the mixtures were added to the target cells directly without washing. After incubation for 48 h, the target cells were harvested, and the quantities of SARS-CoV, baculovirus, or pseudotyped virus were measured by the following three methods: real-time reverse transcription (RT)-PCR for the detection of the open reading frame 1b (ORFIb) and nucleocapsid sequence of SARS-CoV, flow cytometry analysis system (Becton Dickinson, San Jose, CA) for the detection of the EGFP activity in the baculovirus-infected cells, and luciferase activity (Promega, Madison, WI) for the pseudotyped viruses.

To determine the specificity of the interaction, the B-THP-1/DC-SIGN cells were incubated with either mannan (20 μg/ml^{-1}; Sigma-Aldrich), sucrose (20 μg/ml^{-1}; Sigma-Aldrich), EGTA (5 mM; Sigma-Aldrich), anti-L-SIGN MAb 120612 (10 μg/ml^{-1}; R&D Systems), or anti-DC-SIGN MAb 120507 (10 μg/ml^{-1}; R&D Systems) at 37°C for 1 h before the viruses were added to the cultures. In addition, MAbs at different concentrations were also added to the viruses and incubated at 37°C for 1 h before the B-THP-1/DC-SIGN cells or immature DCs were added.

Virus binding assay. B-THP-1 and B-THP-1/DC-SIGN cells (1×10^6) were incubated with variant recombinant baculoviruses (MOI, 10) at 37°C for 2 h. After 2 washings, the cells were incubated with anti-S polyclonal antibody (5) for 30 min. The cells were then washed and incubated with goat anti-rabbit antibody conjugated with fluorescein isothiocyanate (Jackson Immunoresearch, West Grove, Pa.) for 30 min, followed by flow cytometry analysis.

Generation of MAbs against SARS-CoV S protein. Two RPs, SIa and SIb which contains aa residues 1 to 460 and 416 to 846, respectively, were used as antigens to generate MAbs. His-SIb RP was used as a screened antigen to coat an enzyme immunoassay (EIA) plate. The induction and purification procedures of each RP have been described previously (7). Mouse MAbs were produced by a hybridoma technique (31). Briefly, BALB/c mice were immunized with purified RP-SIa or RP-SIb mixed with complete (for primary immunization) or incomplete (for booster injections) Freund adjuvant (Sigma-Aldrich) at 10-day intervals by intraperitoneal injection with a dosage of about 25 μg of RP per inoculum. Three days after the fourth booster, mouse splenocytes were collected and fused with mouse myeloma cell line NS1 (American Type Culture Collection, Rockville, MD) by using polyethylene glycol 1500 (Roche Diagnostics GmbH, Mannheim, Germany). The hybridomas were dispensed into six 96-well plates and cultured in a histone acetyltransferase medium (10). The culture supernatants were screened using EIA with RP-SIa or His-SIb. Hybridoma cells with high optical density were confirmed with Western blot assay immediately. Each well of cells with positive results was subcloned into a 96-well plate with a cell density of 0.5 cell per well. The resultant single clone with positive results was inoculated at a dosage of 5×10^6 to a BALB/c mouse which had been primed with 0.5 ml pristine (Sigma-Aldrich) previously. MAbs were purified from the mouse ascites with protein A antibody purification kits (Pro-Chem, Inc., Acton, MA) and concentrated using Centricon Plus-80 columns (Millipore). The isotype of each MAb was determined using a commercial kit (Southern Biotech, Birmingham, AL).

Synthesis of peptides. The amino acid sequence of the SARS-CoV Urbani strain (38) was used as reference to design 30 synthetic peptides spanning aa 74 to 733 of S protein. The peptides were synthesized using the solid-phase method (Kelowna, Taipei, Taiwan) and dissolved in 5% dimethyl sulfoxide at 2 mg/ml. All peptides are analyzed by high-performance liquid chromatography and mass spectroscopy to verify their identity and stored in lyophilized form at −80°C.

EIA. Different EIAs were designed for the following purposes: to monitor the antibody titers of the immunized animals, to screen for MAbs in the supernatant of different hybridomas, and to determine the reactive epitopes of each monoclonal antibody. Details of the procedures have been described previously (6). Briefly, 100 μl of RP-SIa or His-SIb (5 μg/ml) or synthetic peptides (10 μg/ml) in 0.1 M carbonate buffer (pH 9.6) were added to each well of a 96-well microtiter plate (Corning Costar, Acton, MA) and incubated at 4°C overnight. The antibody titers of mouse serum were determined at a serial 10-fold dilution. For the screening of hybridomas, plates coated with glutathione *S*-transferase (GST) were also used to rule out those MAbs reactive to the GST of the fusion proteins.

WB. Western blot assay (WB) was used to confirm the antibody reactivity of each clone of hybridomas. The RP-SIa (76 kDa in size), RP-SIb (72 kDa in size), and GST (26 kDa in size) were used as the antigens in the WB. After incubating with supernatant of the hybridomas at 37°C for 1 h, the strips were washed for 5 times before reacting with horseradish peroxidase-conjugated goat anti-murine immunoglobulin (Sigma-Aldrich). Then the strips were developed using 3,3′-diaminobenzidine tetrahydrochloride solution (Sigma-Aldrich). The details of the procedures have been described previously (6).

Neutralization assay. For neutralization assay with pseudotyped virus, the HepG2 cells were plated at 1.5×10^5 cells/well in 12-well tissue culture plates

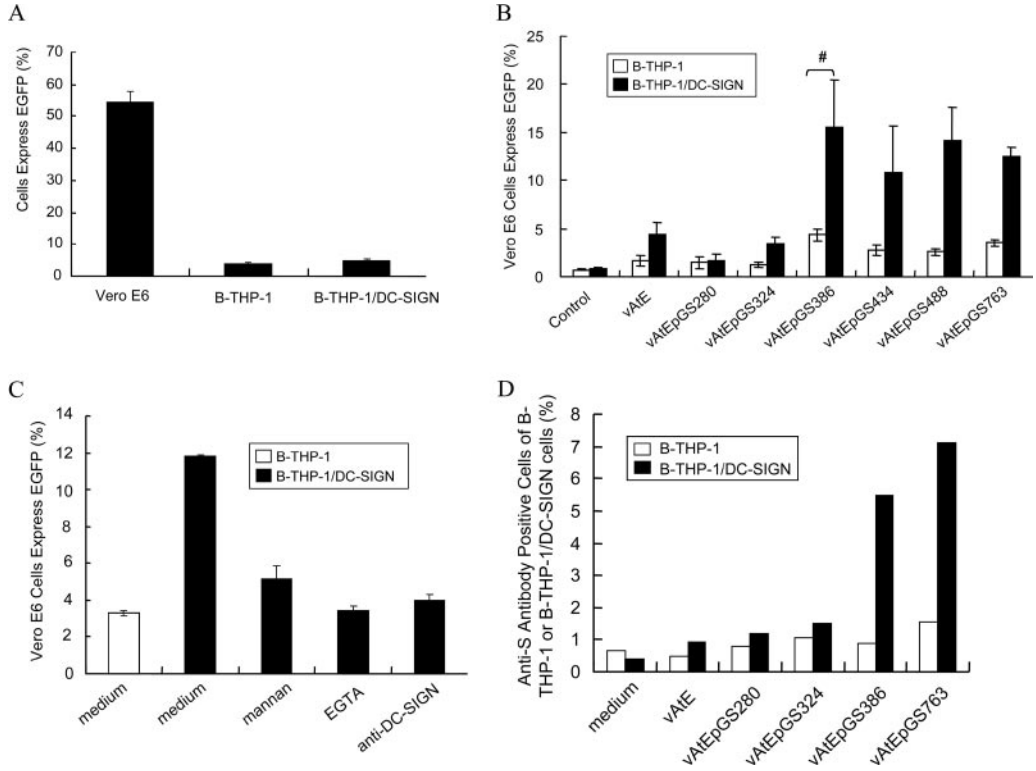

FIG. 1. DC-SIGN binding domain identification in the SARS-CoV S protein using a panel of recombinant baculoviruses. (A) Direct infection assay. A recombinant baculovirus-vAtEpGS763 containing 17 to 763 aa residues of SARS-CoV S protein was used to infect Vero E6, B-THP-1, and B-THP-1/DC-SIGN cells. (B) Capture assay. B-THP-1 or B-THP-1/DC-SIGN cells were incubated with a wild-type virus (vAtE) or a panel of recombinant baculoviruses containing different lengths of SARS-CoV S protein (MOI = 10). After 2 washings, cells were cocultured with Vero E6 cells for 48 h. #, $P < 0.05$, Student's t test. (C) Specificity of the interaction between vAtEpGS386 and DC-SIGN. Recombinant baculovirus vAtEpGS386 was incubated with B-THP-1/DC-SIGN cells in the presence of mannan (20 $\mu g/ml^{-1}$), EGTA (5 mM), or anti-DC-SIGN MAb (10 $\mu g/ml^{-1}$). The unbound virus was eliminated by repeated washings prior to coculture with Vero E6 cells. Infections by recombinant baculoviruses were determined by measuring EGFP expression using flow cytometry. (D) Virus binding assay. B-THP-1 or B-THP-1/DC-SIGN cells were incubated with different recombinant baculoviruses for 2 h before subjected to flow cytometry with anti-S antibody.

and grown overnight. Then, pseudotyped viruses (4 ng of p24 antigen) were incubated with different MAbs (SIb2, SIb4, SIa1, 2, 4, 5, 8, 9, and 10) at 37°C for 1 h before they were added to HepG2 cells. After 48 h, the cell lysates were harvested and the luciferase activity was measured. For neutralization assay with SARS-CoV, Vero E6 cells were plated at 2×10^4 cells/well in 96-well tissue culture plates. SARS-CoV (HKU39849 strain) (3.125 $TCID_{50}$) was mixed with equal volume of MAbs at various dilutions and incubated at 37°C for 1 h before they were added to Vero E6 cells. The cultural supernatant was collected 4 days later, and viral loads were measured using real-time RT-PCR.

Epitope mapping using M13 phage peptide display library. High-titered MAbs purified from ascites were diluted with 0.1 M $NaHCO_3$ (pH 8.6) to a concentration of 100 μg/ml and added to 6-ml sterile polystyrene petri dishes. After coating overnight at 4°C in a humidified container, the plates were blocked with the blocking buffer (0.1 M $NaHCO_3$, pH 8.6, 5 mg/ml bovine serum albumin [BSA], 0.02% NaN_3, with a sterilized filter, stored at 4°C) and incubated for at least 1 h at 4°C. M13 phages displaying random heptapeptides at the N terminus of its minor coat protein (pIII) were subsequently added (Ph.D.-7TM Phage Display Peptide Library; New England Biolabs, Inc.). The phages bound to the plates were selected and repeatedly screened three times before they were subjected to DNA sequencing. Detailed procedures have been published previously (12).

Quantification of SARS-CoV RNA by real-time RT-PCR. Real-time RT-PCR was used to detect the viral signals in the virus infectivity experiment. Viral RNA was extracted from the culture supernatant using the QIAamp viral RNA mini kit (QIAGEN). The following two sets of primers were used in a real-time RT-PCR to measure the viral sequences for nucleocapsid and ORF1b, respectively: CDC-2 forward and reverse primers (CDC catalogue no. KT0051; US CDC) and BNIoutS and BNIoutAs primers (24, 37). For CDC2 primers, the amplification conditions were 48°C for 30 min and 95°C for 10 min, followed by 45 cycles of 95°C for 15 s and 58°C for 1 min. For BNIoutS/BNIoutAs primers, the amplification conditions were 48°C for 30 min and 95°C for 10 min, followed by 50 cycles of 95°C for 15 s and 60°C for 1 min. Reactions were performed using an ABI PRISM 7000 sequence detector (Applied Biosystems). The copy number was determined based on the linear standard curve obtained from the input positive-sense RNA increased from 10 copies to 1,000,000 copies per reaction.

RESULTS

S protein minimal region is interactive with DC-SIGN. Initially, a recombinant baculovirus, vAtEpGS763, containing partial SARS-CoV S protein (aa residues 17 to 763) was used to study its interaction with DC-SIGN. Since the partial S protein was fused with a truncated form of gp64, the major envelope glycoprotein of the baculovirus, it was expressed on the surface of the virus. Three cell lines, Vero E6, B-THP-1, and B-THP-1/DC-SIGN, were tested for their susceptibility to the vAtEpGS763 infection. As shown in Fig. 1A, through measuring the percentages of cells expressing EGFP, we found that about 55% of the Vero E6 cells were infected with vAtEpGS763, while less than 5% of the B-THP-1 and B-THP-1/DC-SIGN cells were susceptible to vAtEpGS763 infection. Subsequently, we used a capture assay to determine whether DC-SIGN is capable of mediating vAtEpGS763 virus to its target cells. Either B-THP-1 or B-THP-1/DC-SIGN cells were

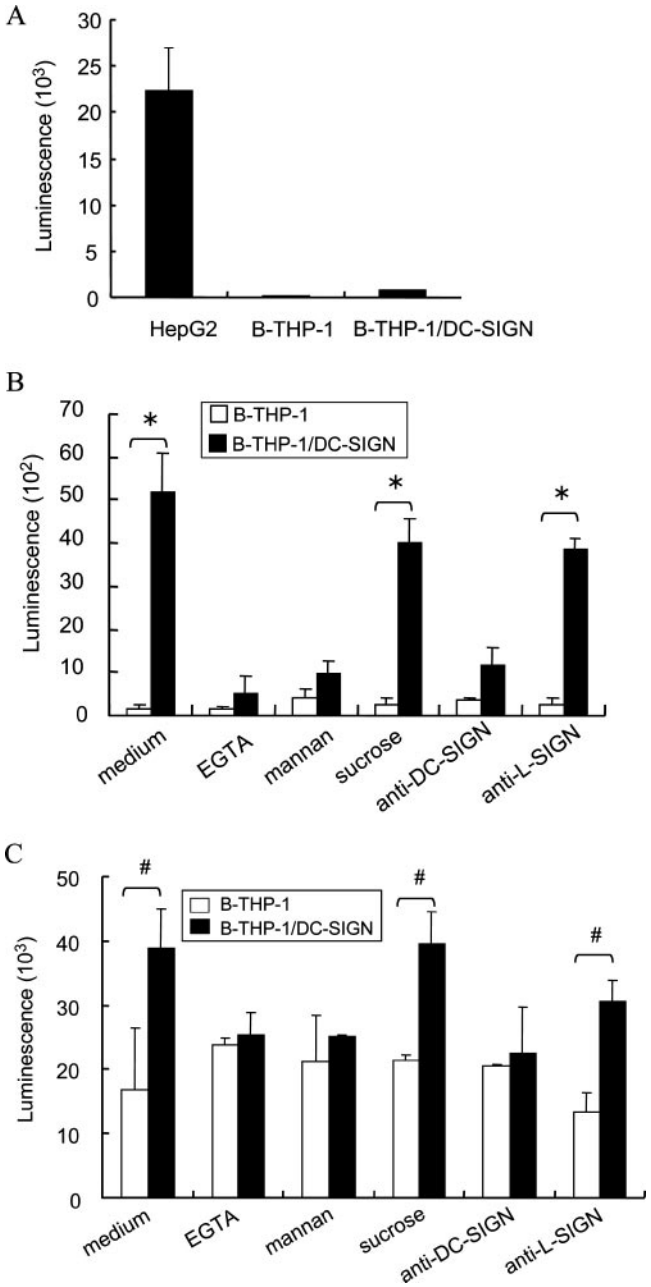

FIG. 2. DC-SIGN not only mediates but also enhances pseudotyped virus infection to HepG2 cells. (A) Direct infection assay. HepG2, B-THP-1, and B-THP-1/DC-SIGN were directly infected with pseudotyped virus equivalent to 4 ng p24 antigen. (B) Capture assay. B-THP-1 or B-THP-1/DC-SIGN cells were incubated with pseudotyped virus for 2 h, washed twice, and then cocultured with HepG2 cells. To study the specificity of the interaction, either B-THP-1 or B-THP-1/DC-SIGN cells were preincubated with mannan (20 $\mu g/ml^{-1}$), sucrose (20 $\mu g/ml^{-1}$), EGTA (5 mM), anti-DC-SIGN MAb (10 $\mu g/ml^{-1}$), or anti-L-SIGN MAb (10 $\mu g/ml^{-1}$) at 37°C for 1 h before the addition of pseudotyped viruses. *, $P < 0.01$, Student's t test. Among all the capture assays with B-THP-1/DC-SIGN (black bars), the luciferase counts of the assays preincubated with EGTA, mannan, or anti-DC-SIGN were significantly lower than that of the medium control ($P < 0.01$). (C) Enhancement assay. B-THP-1 and B-THP-1/DC-SIGN cells were incubated with pseudotyped virus and then cocultured with HepG2 cells without washing. To study the specificity of the enhancement, either B-THP-1 or B-THP-1/DC-SIGN cells were preincubated with mannan (20 $\mu g/ml^{-1}$), sucrose (20 $\mu g/ml^{-1}$), EGTA (5 mM), anti-L-SIGN MAb (10 $\mu g/ml^{-1}$), or anti-DC-SIGN MAb (10 $\mu g/ml^{-1}$) before the addition of pseudotyped viruses. The infectivity was determined 48 h after the infection in the HepG2 cells by measuring the luciferase activity. One representative experiment of two is shown. #, $P < 0.05$, Student's t test.

incubated with the virus for 2 h and washed twice before they were added to the Vero E6 cells. The results showed that, compared to the low percentage (<4%) of vAtEpGS763 infection in the capture assay mediated through B-THP-1, a higher percentage (12%) of the Vero E6 cells were infected by vAtEpGS763 when the mediator was replaced with B-THP-1/DC-SIGN cells (Fig. 1B). The minimal region of the S protein interactive with DC-SIGN was further determined using the following recombinant baculoviruses: vAtEpGS280, vAtEpGS324, vAtEpGS386, vAtEpGS434, and vAtEpGS488. The results showed that only vAtEpGS386, vAtEpGS434, and vAtEpGS488 could be transferred to the target cells via DC-SIGN (Fig. 1B). Since the vAtEpGS386 virus may contain the minimal binding domain for the DC-SIGN, we verified the specificity of their interaction by preincubating B-THP-1/DC-SIGN cells with mannan, EGTA, or an anti-DC-SIGN MAb in the capture assay (Fig. 1C).

We also used flow cytometry analysis to study the direct interaction between the recombinant baculoviruses and DC-SIGN. B-THP-1 or B-THP-1/DC-SIGN cells were incubated with different recombinant baculoviruses for 2 h, and then the cells were washed before they were subjected to flow cytometry with anti-S protein antibodies. As shown in Fig. 1D, all of the recombinant baculoviruses tested did not bind to the B-THP-1 cells. For B-THP-1/DC-SIGN cells, only vAtEpGS386 and vAtEpGS763 viruses showed significantly higher percentages of bindings. Therefore aa residues 324 to 386 of the S protein may contain a DC-SIGN-binding domain.

DC-SIGN mediated and enhanced pseudotyped virus infection of target cells. Besides recombinant baculoviruses, we also used pseudotyped viruses to investigate the interaction between the S protein and its receptors. As shown in Fig. 2A, challenge of B-THP-1 or B-THP-1/DC-SIGN cells with pseudotyped virus resulted only in background levels of luciferase activity. In contrast, HepG2 cells are highly permissive to pseudotyped virus entry. Thus, we employed a standard capture assay to test whether DC-SIGN will mediate the pseudotyped virus to HepG2 cells. Pseudotyped viruses (4 ng of p24 antigen) were added to B-THP-1 or B-THP-1/DC-SIGN cells, and the unbound virus was washed away before the cells were cocultured with HepG2 cells. The results showed that DC-SIGN is capable of mediating the pseudotyped viral infection of HepG2 cells and that this interaction is blocked by mannan, EGTA, and an anti-DC-SIGN MAb but not by anti-L-SIGN MAb or sucrose (Fig. 2B).

To test whether DC-SIGN could enhance SARS-CoV infectivity, a standard enhancement assay was employed. B-THP-1 or B-THP-1/DC-SIGN cells were incubated with pseudotyped virus and then added to HepG2 cells without further washing. The data showed that luciferase activity in HepG2 cells cocultured with B-THP-1/DC-SIGN cells was approximately 2.3-

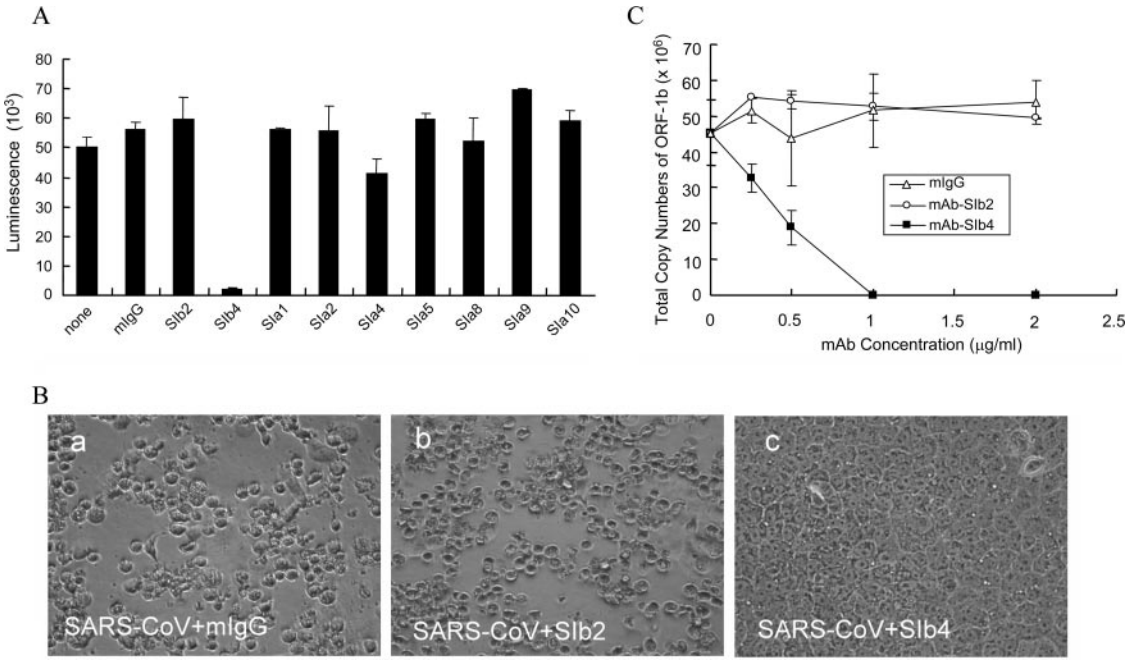

FIG. 3. Neutralizing effect of MAb SIb4. (A) A pseudotyped virus was preincubated with each MAb (15 μg/ml) for 1 h at 37°C prior to infection of HepG2 cells. Infectivity was determined 48 h postinfection by luciferase activity measurement. (B) SARS-CoV strain HKU39849 (3.125 $TCID_{50}$) was incubated with mIgG (a), SIb2 (b), or SIb4 (c) for 1 h at 37°C and then added to Vero E6 cells. Images were taken 96 h postinfection. (C) ORF1b copy numbers in culture supernatant were determined using real-time RT-PCR. Results from one representative experiment of two are shown.

fold higher than that in the HepG2 cells cocultured with B-THP-1 cells. Furthermore, this enhancing effect could be blocked by mannan, EGTA, and an anti-DC-SIGN MAb (Fig. 2C). These results indicate that DC-SIGN not only sequesters SARS-CoV but also enhance SARS-CoV entry to its target cells.

MAb SIb4 had a neutralizing effect. A total of 9 MAbs (7 against RP-SIa and 2 against RP-SIb) were generated for the purpose of mapping the receptor-binding domain. Of all MAbs tested in a pseudotyped virus-neutralization assay, only SIb4 expressed neutralizing activity (Fig. 3A). This was further evaluated using a neutralization assay with the SARS-CoV HKU39849 strain. As shown in Fig. 3B, cytopathic effects (CPE) (including the rounding up and detachment of Vero E6 cells) were observed in cells cultured with viruses preincubated with mouse immunoglobulin G (mIgG) or MAb SIb2 (Fig. 3B-a and 3B-b). In contrast, very little CPE was noted in cells containing viruses treated with MAb SIb4 (Fig. 3B-c). Furthermore, a comparison of SARS-CoV viral loads in culture supernatant showed that among the three antibodies used in the neutralizing assay (SIb4, SIb2, and mIgG), only SIb4 inhibited viral replication. This effect was dose dependent; at a concentration of 1 μg/ml, SIb4 was capable of completely neutralizing viral infectivity (Fig. 3C).

MAb SIa5 inhibited interaction between the S protein and DC-SIGN. A pseudotyped virus capture assay was used to identify which MAbs are capable of blocking the interaction between the S protein and DC-SIGN. Pseudotyped viruses were incubated with different MAbs at 37°C for 1 h before being added to B-THP-1/DC-SIGN cells. After incubation at 37°C for 2 h, cells were washed twice, added to the HepG2 cells, and cocultured for 48 h. Positive results were observed for SIa5 only. Compared to the infectivity of pseudotyped viruses incubated with mIgG, the infectivity of viruses preincubated with MAb SIa5 were reduced nearly 50% (Fig. 4A). These results were confirmed using the HKU39849 SARS-CoV strain in a capture assay. Fifty $TCID_{50}$ of HKU39849 were incubated with MAbs SIa5, SIa10, or mIgG at 37°C for 1 h prior to being added to B-THP-1/DC-SIGN cells. High levels of Vero E6 cell CPE were observed in the mIgG (Fig. 4B-a) and SIa10 (Fig. 4B-b) reactions but not in the SIa5 reaction (Fig. 4B-c). Culture supernatant viral load quantification also demonstrated that only SIa5 was capable of inhibiting viral infectivity; this effect was dose dependent (Fig. 4C).

An enhancement assay with immature dendritic cells purified from a normal donor was employed to measure the blocking effect of MAb SIa5. We mixed 1.625 $TCID_{50}$ of SARS-CoV with either MAb SIa5 or mIgG for 1 h prior to adding to immature DCs and culturing for 2 h. One mixture or the other was added to Vero E6 cells and incubated for another 48 h. Our results indicate extensive CPE in the Vero E6 cells incubated with either SARS-CoV–immature DCs (Fig. 5A-b) or SARS-CoV–immature DCs–mIgG (Fig. 5A-c), and the significantly lower level of CPE in Vero E6 cells incubated with only SARS-CoV (Fig. 5A-a) or SARS-CoV–immature DCs–SIa5 (Fig. 5A-d). Results from culture supernatant quantification indicate that the presence of immature DCs or B-THP-1/DC-SIGN cells enhanced the viral load by approximately 250,000 and 15,000 times, respectively, and that the effect can be blocked by MAb SIa5 but not by mIgG (Fig. 5B).

Reactive epitope mapping for MAbs SIb4 and SIa5. We used an M13 bacteriophage display library to map reactive MAb

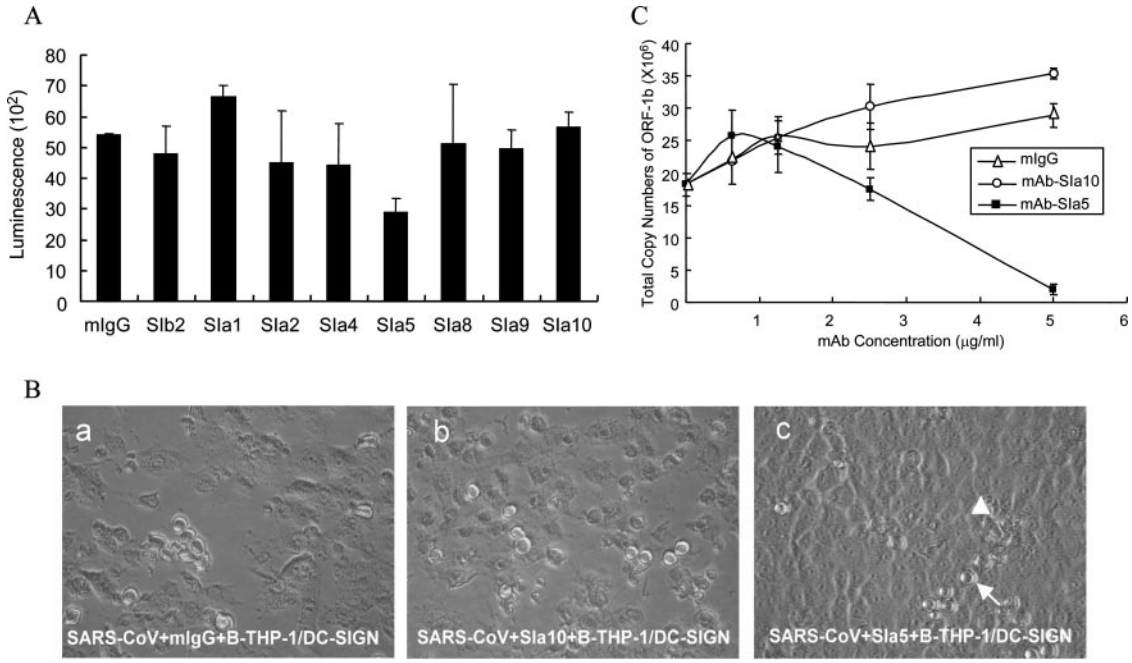

FIG. 4. MAb SIa5 interrupts SARS-CoV S protein interacted with DC-SIGN in a capture assay. (A) Pseudotyped virus was incubated with each MAb (15 μg/ml) for 1 h at 37°C and then incubated with B-THP-1/DC-SIGN cells for 2 h at 37°C. Cells were washed twice and cocultured with HepG2 cells. The luciferase activity in cell lysates was measured 48 h postinfection. The assay with MAb SIa5 had significantly lower luciferase counts than that with mIgG ($P < 0.05$). (B) SARS-CoV (50 $TCID_{50}$) was preincubated with either mIgG (a), SIa10 (b), or SIa5 (c) for 1 h at 37°C, then incubated with B-THP-1/DC-SIGN cells for 2 h at 37°C, washed two times, and added to Vero E6 cells. Images were taken 48 h postinfection. Arrow, B-THP-1/DC-SIGN cells; triangle, Vero E6 cells. (C) Infectivity was determined by measuring the copy numbers of ORF1b mRNA in culture supernatant. Results from one representative experiment of two are shown.

epitopes and found that 3 of the 9 epitopes could not be determined using this method (Table 1). Deduced consensus sequences for SIb4 and SIa5 epitopes were NYNWK (aa 435 to 439) and TFKCYG (aa 363 to 368), respectively.

We also employed peptide scanning for epitope mapping, initially using 14 synthetic peptides (SPs, 50 aa in length) spanning S protein aa residues 74 to 733 in EIAs. Our results indicate that MAb SIa5 reacted with both SP-324-373 and SP-364-413 and that MAb SIb4 had a relatively high optical density in its reaction with SP-404-453 (Fig. 6A). We therefore performed additional peptide scans with shorter (15 aa) synthetic peptides spanning aa 324 to 413 and aa 404 to 453. Reactive epitopes for SIa5 and SIb4 were identified in aa residues 359 to 373 and 434 to 448, respectively (Fig. 6C and B, respectively).

A direct infection assay test using SP-434-448 was performed to determine its capability to block pseudotyped viral infections. As shown in Fig. 6D, SP-434-448 inhibited pseudotyped viral infection at concentrations of 10 μg/ml (33%) and 20 μg/ml (59%). Neither SP-175-205 nor OC43-SP-186-200 (a peptide containing aa residues 186 to 200 of the OC43 coronavirus S protein) significantly inhibited pseudotyped viral infection.

Determining N-linked glycosylation sites responsible for interaction between S glycoprotein and DC-SIGN. After identifying Sla5 reactive epitopes near two N-glycosylation sites (N330 and N357), we set out to determine whether these sites affect DC-SIGN binding by generating four pseudotyped viruses with amino acid residue mutations for the capture assay. Compared to the wild-type and N65Q pseudotyped viruses, the DC-SIGN-binding capacity of the N330Q, N357Q, or N330Q plus N357Q double mutant pseudotyped viruses was reduced about 50% to 60% (Fig. 6E). We therefore suggest that residues N330 and N357 of the S protein may play important roles for interaction between the S glycoprotein and DC-SIGN.

DISCUSSION

DC-SIGN binding to pathogens depends on the presence of high-mannose N-linked carbohydrate chains or fucosylated oligosaccharides on the pathogen surface (20). We initially used recombinant baculoviruses to map minimal regions on the SARS-CoV S protein for DC-SIGN binding and identified a region between aa residues 324 and 386. In this study, the recombinant baculovirus may infect Vero E6 cells using other receptors besides ACE2. However, in the capture assay, only baculoviruses that can bind to DC-SIGN will be transferred to the Vero E6 cells. Therefore, whether Vero cells infection can be blocked by antibody against ACE2 will not affect the results shown in Fig. 1B. Since there are only two N-linked glycosylation sites in this region, we generated N330Q and N357Q pseudotype virus mutants to study S protein–DC-SIGN interaction and found that both mutants reduce their DC-SIGN binding capacity. However, the DC-SIGN binding capacity cannot be completely abolished using a N330Q plus N357Q double mutant pseudotyped virus in the capture assay (Fig. 6E). It suggests that DC-SIGN may interact with other carbohydrate chains on the S glycoprotein.

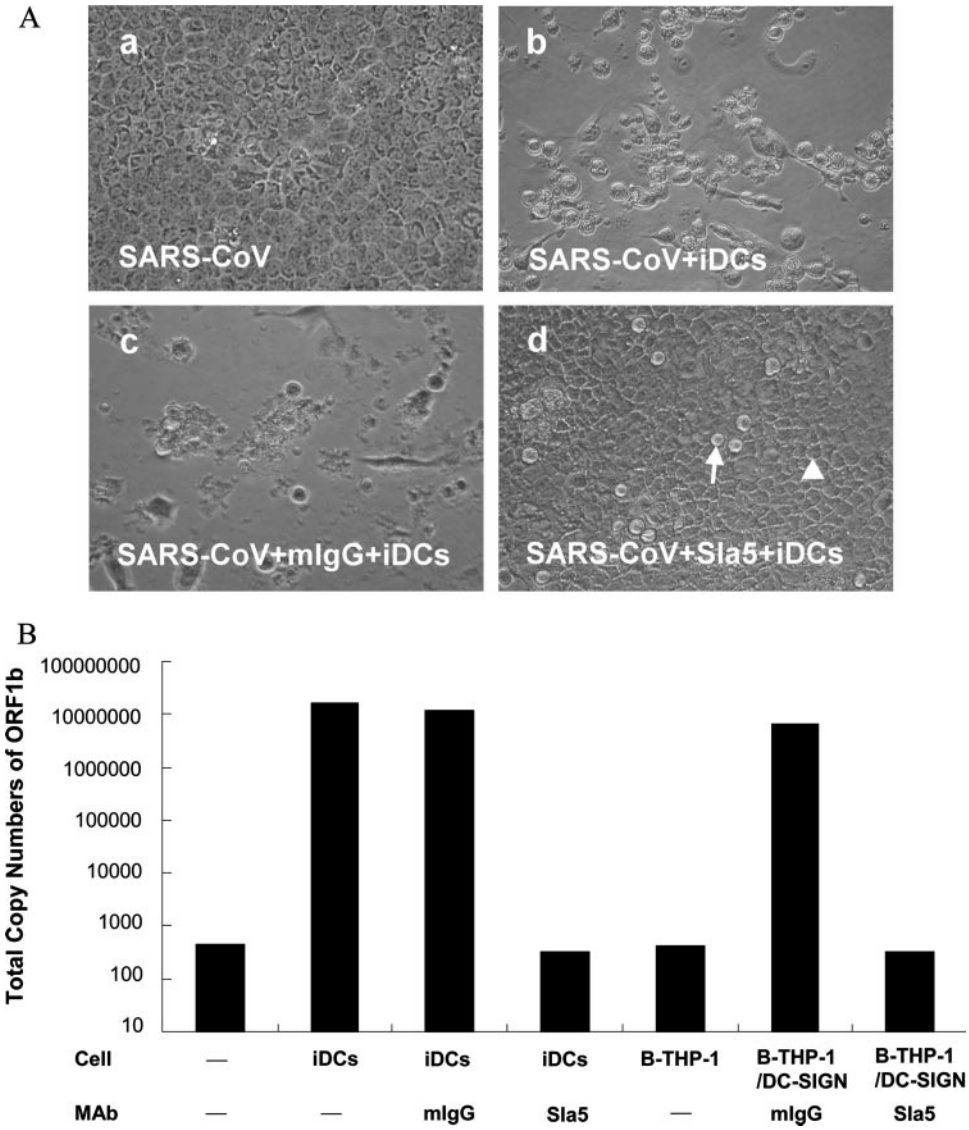

FIG. 5. MAb SIa5 interrupts SARS-CoV S protein interacted with DC-SIGN in an enhancement assay. (A) SARS-CoV (1.625 $TCID_{50}$) was mixed with no antibody (b), mIgG (c), or SIa5 (5 μg/ml) (d) for 1 h before being added to immature DCs (iDCs) and cultured for 2 h. Cells were not washed prior to being added to Vero E6 cells. Alternative (a) shows Vero E6 cells directly infected with the SARS-CoV. Images were taken 96 h postinfection. Arrow, B-THP-1/DC-SIGN cells; triangle, Vero E6 cells. (B) Infectivity was determined by measuring the copy numbers of ORF1b mRNA in cultural supernatant. Results from one representative experiment of two are shown.

Recombinant baculovirus infection rates in a capture assay were low (10 to 15%), and a flow cytometry analysis of EGFP in the baculovirus system is less distinguishable than the luciferase assay. We therefore decided to use a pseudotyped virus system to screen a panel of MAbs against the SARS-CoV S protein. Our results indicate that MAb SIb4 was capable of neutralizing SARS-CoV infectivity in vitro; its reactive epitope was traced to aa residues 435 to 439 of the S protein. This result is consistent with Li et al.'s previous identification of a minimal ACE2 receptor-binding motif of the S protein at aa residues 424 to 494 (29). Furthermore, results from an assay of the inhibitory effect of SP-434-448 on pseudotyped virus infectivity show that it was capable of blocking the entry of a pseudotyped virus into HepG2 cells (Fig. 6D). He et al. reported a lack of neutralizing activity for MAb 4D5 (with an epitope mapped to aa residues 435 to 451) (22). We therefore suggest that the MAb 4D5 reactive epitope may reside in a region between aa residues 440 and 451 of the S protein.

We generated MAb SIb4 by immunizing BALB/c mice with glutathione *S*-transferase–SIb fusion protein produced from *Escherichia coli*. Hybridomas were screened using EIA plates coated with His-tagged SIb RP. This approach differs from methods used in other laboratories. Traggiai et al. used the Epstein-Barr virus to immortalize B lymphocytes from SARS-CoV-infected patients and used EIAs coated with sodium dodecyl sulfate-extracted viral proteins to screen for MAbs. Neutralizing activity was observed for a human MAb S3.1, but its reactive epitope was not identified (42). Chou et al. immunized BALB/c mice with inactive SARS-CoV–BJ01 virus particles and used EIAs coated with inactive viruses to

TABLE 1. Epitopes and Ig subtypes of MAbs against the S protein of SARS-CoV

MAb	Epitope[a]	Result for Ig subtype							
		Heavy chain						Light chain	
		IgG1	IgG2a	IgG2b	IgG3	IgA	IgM	κ	λ
SIa1	^{58}N**FLP**RP^{63}	−	−	+	−	−	−	+	−
SIa2	NI*	+	−	−	−	−	−	+	−
SIa4	^{58}**P**F**LP**RP^{63}	+	−	−	−	−	−	+	−
SIa5	^{363}**TF**LARG^{368}	−	−	+	−	−	−	+	−
SIa8	NI*	+	−	−	−	−	−	+	−
SIa9	^{449}**RP**SK**R**P^{454}	+	−	−	−	−	−	+	−
SIa10	^{58}**LFLP**RV^{63}	+	−	−	−	−	−	+	−
SIb2	NI*	+	−	−	−	−	−	+	−
SIb4	^{435}**NYN**W**K**R^{440}	+	−	−	−	−	−	+	−

[a] MAbs were screened with a phage display library as described in Materials and Methods. Boldface and underlined residues represent identities. The numbers indicate the locations of the epitopes on the S protein. *, not identified.

screen for MAbs. Using EIAs coated with seven different RPs, they mapped the epitopes of two MAbs with neutralizing power (1A5 and 2C5) to aa residues 310 to 535 (9). He et al. used a recombinant fusion protein produced in a mammalian cell culture system (aa residues 318 to 510 of the S protein linked to the Fc domain of human IgG1) as an immunogen and screened for MAbs using SI RP. They obtained 27 MAbs, 23 of which showed neutralizing activity.

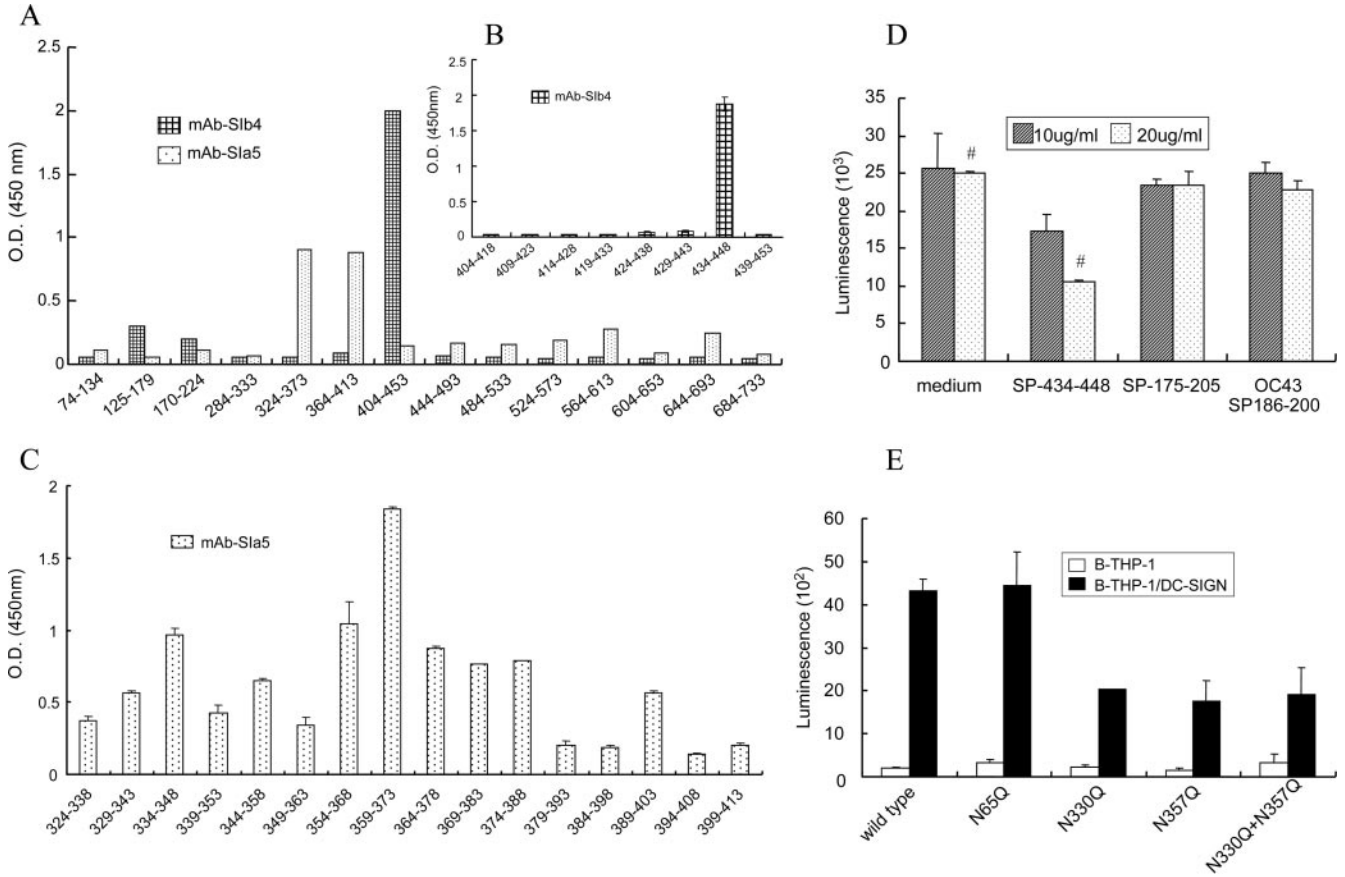

FIG. 6. Results of peptide scan for MAbs SIb4 and SIa5. (A) EIAs with 14 SPs, each 50 aa in length, were employed in the study. OD, optical density. (B) EIAs with 8 SPs (each 15 aa in length) were used for MAb SIb4 epitope mapping. (C) EIAs with 16 SPs (each 15 aa in length) were used for MAb SIa5 epitope mapping. (D) Inhibitory effect of SP-434-448 on pseudotyped virus infectivity. Prior to pseudotyped viral infection, HepG2 cells were incubated with SP-434-448, SP-175-205, or OC43-SP-186-200 for 1 h. Infectivity was determined 2 days postinfection by measuring luciferase activity. Results from one representative experiment of two are shown. #, the difference of the luciferase counts between these two reactions was statistically significant ($P < 0.05$). (E) A lack of glycosylation impaired the ability of the S protein to bind to DC-SIGN. Either B-THP-1 or B-THP-1/DC-SIGN cells were incubated with different pseudotyped viruses for 2 h at 37°C. Cells were washed twice and cocultured with HepG2 cells. Infectivity was determined after 48 h by measuring luciferase activity.

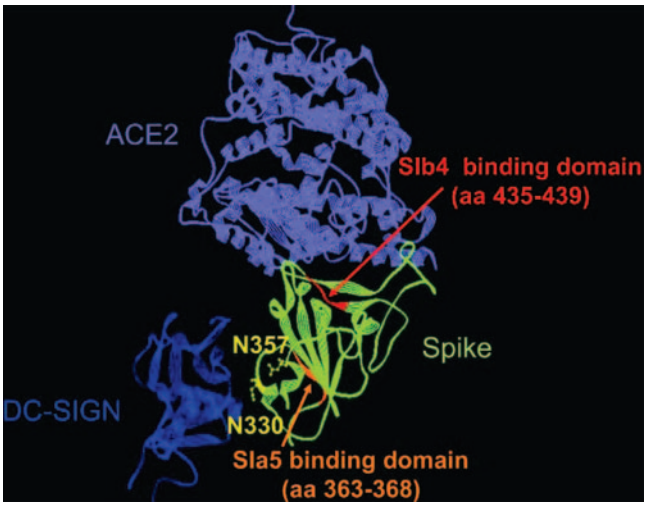

FIG. 7. Different S protein binding domains for ACE2 and DC-SIGN. Schematic diagram of ACE2 (purple), the carbohydrate recognition domain of DC-SIGN (blue), and binding sites in the receptor binding domain (green) of the SARS-CoV spike protein. Red, MAb SIb4-recognized epitope; orange, MAb SIa5-recognized epitope; yellow, N-glycosylation sites N330 and N357 (modified from reference 29).

Unfortunately, all 23 reacted with conformational epitopes (22).

All of the methods just mentioned are capable of generating neutralizing MAbs that either recognize conformational epitopes or react with a broader region than that recognized by the MAb SIb4 epitope. This discrepancy may be due to differences in the immunogen productive systems or MAb screening systems. The GST portion of the fusion protein used for the immunization protocol in this study exerted a stabilizing effect on the GST-SIa RP. In the absence of posttranslational modification, it may be easier to induce antibodies against linear epitopes. Moreover, the antigen used in our EIAs (His-tagged SI protein) for MAb screening did not contain a GST portion of the immunogen; therefore, this system will not detect anti-GST MAbs.

According to our data, both B-THP-1/DC-SIGN cells and immature DCs are capable of capturing the SARS-CoV and enhancing the viral infection. This finding is consistent with those reported by other laboratories (33, 44). The difference is that the present study used SARS-CoV. When we challenged Vero E6 cells with relatively low titers of SARS-CoV (e.g., 1.625 $TCID_{50}$ in the enhancement assay), the results showed a 15,000-fold increase in viral infection due to B-THP-1/DC-SIGN cells (Fig. 5B) and a 250,000-fold viral infection enhancement by immature DCs. To understand this significant difference, we used flow cytometry to compare DC-SIGN expression levels between B-THP-1/DC-SIGN cells and immature DCs and found a much higher mean fluorescent intensity for DC-SIGN detected in immature DCs (893 versus 589 for B-THP-1/DC-SIGN cells) (data not shown). This suggests that the role of DC-SIGN in SARS-CoV infection enhancement should not be underestimated. Our results point to a significant inhibitory effect of MAb SIa5 in capture and enhancement assays but a lack of neutralizing effect in a direct infection assay. In other words, SIa5 reacts to the DC-SIGN binding domain but not to the ACE2 binding domain. The MAb SIa5 reactive epitope was mapped to aa residues 363 to 368 of the S protein using both peptide scan and phage display methods. This matches our results obtained from the baculovirus system—that is, a DC-SIGN binding domain in aa residues 324 to 386 of the S protein. As shown in Fig. 7, we used an X-ray crystallography of ACE2 and the receptor binding domain of S protein (29) to demonstrate the spatial relationship between the MAb SIa5 and SIb4 reactive epitopes. In the figure, two N-linked glycosylation sites (N330 and N357) that affect the interaction between the S protein and DC-SIGN were found to be very close to the SIa5 binding domain. It is therefore reasonable to imagine that once MAb SIa5 binds to the S protein, it is capable of blocking interaction between the S protein and DC-SIGN. Since these two N-linked glycosylation sites are located not very far from the ACE2-binding domain, we suggest that the binding of the DC-SIGN may induce a conformational change of the S protein, which results in more efficient interaction with its ACE2 receptor.

This is the first time a linear epitope and two N-linked glycosylation sites have been identified as being associated with DC-SIGN interaction. The model may be valuable for studying interactions between DC-SIGN and other pathogens—for instance, HIV-1.

ACKNOWLEDGMENTS

We thank Michael Farzan for providing the pcDNA3 codon-optimal S plasmid, the Taiwan Center for Disease Control for providing samples of SARS-CoV-TWC viral RNA and the SARS-CoV HKU39849 strain, and Vineet KewalRamani for providing B-THP-1/DC-SIGN cells and for his helpful discussions.

This work was supported in part by a grant from the National Science Council of Taiwan (no. NSC 92-2751-B010-001Y).

REFERENCES

1. **Aden, D. P., A. Fogel, S. Plotkin, I. Damjanov, and B. B. Knowles.** 1979. Controlled synthesis of HBsAg in a differentiated human liver carcinoma-derived cell line. Nature **282:**615–616.
2. **Alvarez, C. P., F. Lasala, J. Carrillo, O. Muniz, A. L. Corbi, and R. Delgado.** 2002. C-type lectins DC-SIGN and L-SIGN mediate cellular entry by Ebola virus in *cis* and in *trans*. J. Virol. **76:**6841–6844.
3. **Bashirova, A. A., T. B. H. Geijtenbeek, G. C. F. van Duijnhoven, S. J. van Vliet, J. B. G. Eilering, M. P. Martin, L. Wu, T. D. Martin, N. Viebig, P. A. Knolle, V. N. KewalRamani, Y. van Kooyk, and M. Carrington.** 2001. A dendritic cell-specific intercellular adhesion molecule 3-grabbing nonintegrin (DC-SIGN)-related protein is highly expressed on human liver sinusoidal endothelial cells and promotes HIV-1 infection. J. Exp. Med. **193:**671–678.
4. **Chan, V. S. F., K. Y. K. Chan, Y. Chen, L. L. M. Poon, A. N. Y. Cheung, B. Zheng, K. H. Chan, W. Mak, H. Y. S. Ngan, X. Xu, G. Screaton, P. K. H. Tam, J. M. Austyn, L. C. Chan, S. P. Yip, M. Peiris, U. S. Khoo, and C. L. Lin.** 2006. Homozygous L-SIGN (CLEC4M) plays a protective role in SARS coronavirus infection. Nat. Genet. **38:**38–46.
5. **Chang, Y. J., C. Y. Y. Liu, B. L. Chiang, Y. C. Chao, and C. C. Chen.** 2004. Induction of IL-8 release in lung cells via activator protein-1 by recombinant baculovirus displaying severe acute respiratory syndrome-coronavirus spike proteins: identification of two functional regions. J. Immunol. **173:**7602–7614.
6. **Chen, Y. M., X. Q. Zhang, C. E. Dahl, K. P. Samuel, R. T. Schooley, M. Essex, and T. S. Papas.** 1991. Delineation of type-specific regions on the envelope glycoproteins of human T cell leukemia viruses. J. Immunol. **147:**2368–2376.
7. **Chen, Y. M. A., S. Y. Liang, Y. P. Shih, C. Y. Chen, Y. M. Lee, L. Chang, S. Y. Jung, M. S. Ho, K. Y. Liang, H. Y. Chen, Y. J. Chan, and D. C. Chu.** 2006. Epidemiological and genetic correlates of severe acute respiratory syndrome coronavirus infection in the hospital with the highest nosocomial infection rate in Taiwan in 2003. J. Clin. Microbiol. **44:**359–365.
8. **Chen, Z., L. Zhang, C. Qin, L. Ba, C. E. Yi, F. Zhang, Q. Wei, T. He, W. Yu, J. Yu, H. Gao, X. Tu, A. Gettie, M. Farzan, K.-Y. Yuen, and D. D. Ho.** 2005. Recombinant modified vaccinia virus Ankara expressing the spike glycopro-

tein of severe acute respiratory syndrome coronavirus induces protective neutralizing antibodies primarily targeting the receptor binding region. J. Virol. **79:**2678–2688.
9. **Chou, T. H., S. Wang, P. V. Sakhatskyy, I. Mboudoudjeck, J. M. Lawrence, S. Huang, S. Coley, B. Yang, J. Li, Q. Zhu, and S. Lu.** 2005. Epitope mapping and biological function analysis of antibodies produced by immunization of mice with an inactivated Chinese isolate of severe acute respiratory syndrome-associated coronavirus (SARS-CoV). Virology **334:**134–143.
10. **Chu, T. M., E. Kawinski, and T. H. Lin.** 1993. Characterization of a new monoclonal antibody F4 detecting cell surface epitope and P-glycoprotein in drug-resistant human tumor cell lines. Hybridoma **12:**417–429.
11. **Connor, R. I., B. K. Chen, S. Choe, and N. R. Landau.** 1995. Vpr is required for efficient replication of human immunodeficiency virus type-1 in mononuclear phagocytes. Virology **206:**935–944.
12. **Cortese, R. F., P. F. Monaci, A. F. Luzzago, C. F. Santini, F. F. Bartoli, I. F. Cortese, P. F. Fortugno, G. F. Galfre, A. F. Nicosia, and F. Felici.** 1996. Selection of biologically active peptides by phage display of random peptide libraries. Curr. Opin. Biotechnol. **7:**616–621.
13. **Curtis, B. M., S. Scharnowski, and A. J. Watson.** 1992. Sequence and expression of a membrane-associated C-type lectin that exhibits CD4-independent binding of human immunodeficiency virus envelope glycoprotein gp120. Proc. Natl. Acad. Sci. USA **89:**8356–8360.
14. **Donnelly, C. A., A. C. Ghani, G. M. Leung, A. J. Hedley, C. Fraser, S. Riley, L. J. bu-Raddad, L. M. Ho, T. Q. Thach, and P. Chau.** 2003. Epidemiological determinants of spread of causal agent of severe acute respiratory syndrome in Hong Kong. Lancet **361:**1761–1766.
15. **Drosten, C., S. Gunther, W. Preiser, S. van der Werf, H. R. Brodt, S. Becker, H. Rabenau, M. Panning, L. Kolesnikova, R. A. M. Fouchier, A. Berger, A. M. Burguiere, J. Cinatl, M. Eickmann, N. Escriou, K. Grywna, S. Kramme, J. C. Manuguerra, S. Muller, V. Rickerts, M. Sturmer, S. Vieth, H. D. Klenk, A. D. M. E. Osterhaus, H. Schmitz, and H. W. Doerr.** 2003. Identification of a novel coronavirus in patients with severe acute respiratory syndrome. N. Engl. J. Med. **348:**1967–1976.
16. **Engering, A., T. B. H. Geijtenbeek, S. J. van Vliet, M. Wijers, E. van Liempt, N. Demaurex, A. Lanzavecchia, J. Fransen, C. G. Figdor, V. Piguet, and Y. van Kooyk.** 2002. The dendritic cell-specific adhesion receptor DC-SIGN internalizes antigen for presentation to T cells. J. Immunol. **168:**2118–2126.
17. **Fouchier, R. A. M., T. Kuiken, M. Schutten, G. van Amerongen, G. J. J. van Doornum, B. G. van den Hoogen, M. Peiris, W. Lim, K. Stohr, and A. D. M. E. Osterhaus.** 2003. Aetiology: Koch's postulates fulfilled for SARS virus. Nature **423:**240.
18. **Geijtenbeek, T. B. H., D. S. Kwon, R. Torensma, S. J. van Vliet, G. C. F. van Duijnhoven, J. Middel, I. L. M. H. Cornelissen, H. S. L. M. Nottet, V. N. KewalRamani, and D. R. Littman.** 2000. DC-SIGN, a dendritic cell-specific HIV-1-binding protein that enhances trans-infection of T Cells. Cell **100:**587–597.
19. **Graham, F. L., J. Smiley, W. C. Russell, and R. Nairn.** 1977. Characteristics of a human cell line transformed by DNA from human adenovirus type 5. J. Gen. Virol. **36:**59–74.
20. **Guo, Y., H. Feinberg, E. Conroy, D. A. Mitchell, R. Alvarez, O. Blixt, M. E. Taylor, W. I. Weis, and K. Drickamer.** 2004. Structural basis for distinct ligand-binding and targeting properties of the receptors DC-SIGN and DC-SIGNR. Nat. Struct. Mol. Biol. **11:**591–598.
21. **Halary, F., A. Amara, H. Lortat-Jacob, M. Messerle, T. Delaunay, C. Houles, F. Fieschi, F. Renzana-Seisdedos, J. F. Moreau, and J. Chanet-Merville.** 2002. Human cytomegalovirus binding to DC-SIGN is required for dendritic cell infection and target cell trans-infection. Immunity **17:**653–664.
22. **He, Y., H. Lu, P. Siddiqui, Y. Zhou, and S. Jiang.** 2005. Receptor-binding domain of severe acute respiratory syndrome coronavirus spike protein contains multiple conformation-dependent epitopes that induce highly potent neutralizing antibodies. J. Immunol. **174:**4908–4915.
23. **Jeffers, S. A., S. M. Tusell, L. Gillim-Ross, E. M. Hemmila, J. E. Achenbach, G. J. Babcock, W. D. Thomas, Jr., L. B. Thackray, M. D. Young, R. J. Mason, D. M. Ambrosino, D. E. Wentworth, J. C. DeMartini, and K. V. Holmes.** 2004. CD209L (L-SIGN) is a receptor for severe acute respiratory syndrome coronavirus. Proc. Natl. Acad. Sci. USA **101:**15748–15753.
24. **Jiang, S. S., T. C. Chen, J. Y. Yang, C. A. Hsiung, I. J. Su, Y. L. Liu, P. C. Chen, and J. L. Juang.** 2003. Sensitive and quantitative detection of severe acute respiratory syndrome coronavirus infection by real-time nested polymerase chain reaction. Clin. Infect. Dis. **38:**293–296.
25. **Kitamura, T., C. Morita, T. Komatsu, K. Sugiyama, J. Arikawa, S. Shiga, H. Takeda, Y. Akao, K. Imaizumi, A. Oya, N. Hashimoto, and S. Urasawa.** 1983. Isolation of virus causing hemorrhagic fever with renal syndrome (HFRS) through a cell culture system. Jpn. J. Med. Sci. Biol. **36:**17–25.
26. **Ksiazek, T. G., D. Erdman, C. S. Goldsmith, S. R. Zaki, T. Peret, S. Emery, S. Tong, C. Urbani, J. A. Comer, W. Lim, P. E. Rollin, S. F. Dowell, A. E. Ling, C. D. Humphrey, W. J. Shieh, J. Guarner, C. D. Paddock, P. Rota, B. Fields, J. DeRisi, J. Y. Yang, N. Cox, J. M. Hughes, J. W. LeDuc, W. J. Bellini, L. J. Anderson, and the SARS Working Group.** 2003. A novel coronavirus associated with severe acute respiratory syndrome. N. Engl. J. Med. **348:**1953–1966.
27. **Kwon, D. S., G. Gregorio, N. Bitton, W. A. Hendrickson, and D. R. Littman.** 2002. DC-SIGN-mediated internalization of HIV is required for trans-enhancement of T cell infection. Immunity **16:**135–144.
28. **Lan, Y. C., H. F. Liu, Y. P. Shih, J. Y. Yang, H. Y. Chen, and Y. M. A. Chen.** 2005. Phylogenetic analysis and sequence comparisons of structural and non-structural SARS coronavirus proteins in Taiwan. Infect. Genet. Evol. **5:**261–269.
29. **Li, F., W. Li, M. Farzan, and S. C. Harrison.** 2005. Structure of SARS coronavirus spike receptor-binding domain complexed with receptor. Science **309:**1864–1868.
30. **Li, W., M. J. Moore, N. Vasilieva, J. Sui, S. K. Wong, M. A. Berne, M. Somasundaran, J. L. Sullivan, K. Luzuriaga, T. C. Greenough, H. Choe, and M. Farzan.** 2003. Angiotensin-converting enzyme 2 is a functional receptor for the SARS coronavirus. Nature **426:**450–454.
31. **Liu, H. H., K. H. Chen, Y. P. Shih, W. Y. Lui, F. Wong, and Y. M. A. Chen.** 2003. Characterization of reduced expression of glycine N-methyltransferase in cancerous hepatic tissues using two newly developed monoclonal antibodies. J. Biomed. Sci. **10:**87–97.
32. **Lozach, P. Y., A. Amara, B. Bartosch, J. L. Virelizier, F. Renzana-Seisdedos, F. L. Cosset, and R. Altmeyer.** 2004. C-type lectins L-SIGN and DC-SIGN capture and transmit infectious hepatitis C virus pseudotype particles. J. Biol. Chem. **279:**32035–32045.
33. **Marzi, A., T. Gramberg, G. Simmons, P. Moller, A. J. Rennekamp, M. Krumbiegel, M. Geier, J. Eisemann, N. Turza, B. Saunier, A. Steinkasserer, S. Becker, P. Bates, H. Hofmann, and S. Pohlmann.** 2004. DC-SIGN and DC-SIGNR interact with the glycoprotein of Marburg virus and the S protein of severe acute respiratory syndrome coronavirus. J. Virol. **78:**12090–12095.
34. **Mitchell, D. A., A. J. Fadden, and K. Drickamer.** 2001. A novel mechanism of carbohydrate recognition by the C-type lectins DC-SIGN and DC-SIGNR. Subunit organization and binding to multivalent ligands. J. Biol. Chem. **276:**28939–28945.
35. **Peiris, J. S. M., S. T. Lai, L. L. M. Poon, Y. Guan, L. Y. C. Yam, W. Lim, J. Nicholls, W. K. S. Yee, W. W. Yan, and M. T. Cheung.** 2003. Coronavirus as a possible cause of severe acute respiratory syndrome. Lancet **361:**1319–1325.
36. **Pohlmann, S., J. Zhang, F. Baribaud, Z. Chen, G. J. Leslie, G. Lin, A. Granelli-Piperno, R. W. Doms, C. M. Rice, and J. A. McKeating.** 2003. Hepatitis C virus glycoproteins interact with DC-SIGN and DC-SIGNR. J. Virol. **77:**4070–4080.
37. **Poon, L. L. M., K. H. Chan, O. K. Wong, T. K. W. Cheung, I. Ng, B. Zheng, W. H. Seto, K. Y. Yuen, Y. Guan, and J. S. M. Peiris.** 2004. Detection of SARS coronavirus in patients with severe acute respiratory syndrome by conventional and real-time quantitative reverse transcription-PCR assays. Clin. Chem. **50:**67–72.
38. **Rota, P. A., M. S. Oberste, S. S. Monroe, W. A. Nix, R. Campagnoli, J. P. Icenogle, S. Penaranda, B. Bankamp, K. Maher, M. H. Chen, S. Tong, A. Tamin, L. Lowe, M. Frace, J. L. DeRisi, Q. Chen, D. Wang, D. D. Erdman, T. C. T. Peret, C. Burns, T. G. Ksiazek, P. E. Rollin, A. Sanchez, S. Liffick, B. Holloway, J. Limor, K. McCaustland, M. Olsen-Rasmussen, R. Fouchier, S. Gunther, A. D. M. E. Osterhaus, C. Drosten, M. A. Pallansch, L. J. Anderson, and W. J. Bellini.** 2003. Characterization of a novel coronavirus associated with severe acute respiratory syndrome. Science **300:**1394–1399.
39. **Soilleux, E. J., R. Barten, and J. Trowsdale.** 2000. Cutting edge: DC-SIGN; a related gene, DC-SIGNR; and CD23 form a cluster on 19p13. J. Immunol. **165:**2937–2942.
40. **Spiga, O., A. Bernini, A. Ciutti, S. Chiellini, N. Menciassi, F. Finetti, V. Causarono, F. Anselmi, F. Prischi, and N. Niccolai.** 2003. Molecular modelling of S1 and S2 subunits of SARS coronavirus spike glycoprotein. Biochem. Biophys. Res. Commun. **310:**78–83.
41. **Tassaneetrithep, B., T. H. Burgess, A. Granelli-Piperno, C. Trumpfheller, J. Finke, W. Sun, M. A. Eller, K. Pattanapanyasat, S. Sarasombath, D. L. Birx, R. M. Steinman, S. Schlesinger, and M. A. Marovich.** 2003. DC-SIGN (CD209) mediates Dengue virus infection of human dendritic cells. J. Exp. Med. **197:**823–829.
42. **Traggiai, E., S. Becker, K. Subbarao, L. Kolesnikova, B. Uematsu, M. R. Gismondo, B. R. Murphy, R. Rappuoli, and A. Lanzavecchia.** 2004. An efficient method to make human monoclonal antibodies from memory B cells: potent neutralization of SARS coronavirus. Nat. Med. **10:**871–875.
43. **Wu, L., T. D. Martin, M. Carrington, and V. N. KewalRamani.** 2004. Raji B cells, misidentified as THP-1 cells, stimulate DC-SIGN-mediated HIV transmission. Virology **318:**17–23.
44. **Yang, Z. Y., Y. Huang, L. Ganesh, K. Leung, W. P. Kong, O. Schwartz, K. Subbarao, and G. J. Nabel.** 2004. pH-dependent entry of severe acute respiratory syndrome coronavirus is mediated by the spike glycoprotein and enhanced by dendritic cell transfer through DC-SIGN. J. Virol. **78:**5642–5650.
45. **Zeng, F. Y., C. W. M. Chan, M. N. Chan, J. D. Chen, K. Y. C. Chow, C. C. Hon, K. H. Hui, J. Li, V. Y. Y. Li, C. Y. Wang, P. Y. Wang, Y. Guan, B. Zheng, L. L. M. Poon, K. H. Chan, K. Y. Yuen, J. S. M. Peiris, and F. C. Leung.** 2003. The complete genome sequence of severe acute respiratory syndrome coronavirus strain HKU-39849 (HK-39). Exp. Biol. Med. **228:**866–873.